

Magnetic tunnel junction field sensors with hard-axis bias field

Xiaoyong Liu,^{a)} Cong Ren, and Gang Xiao

Department of Physics, Brown University, Providence, Rhode Island 02912

(Received 12 April 2002; accepted for publication 23 July 2002)

We have fabricated and studied the magnetic properties of the $\text{Ni}_{81}\text{Fe}_{19}/\text{Al}_2\text{O}_3/\text{Ni}_{81}\text{Fe}_{19}$ based magnetic tunnel junction sensors. Magnetoresistance (MR) of 35% is achieved with a small applied field (<10 Oe). The introduction of a hard axis bias field linearizes the MR response. The hysteresis disappears in hard-axis fields greater than 3 Oe, which corresponds to the effective anisotropy field along the easy axis. A sensitivity of 3.5%/Oe has been demonstrated in this linear region. Low-frequency noise measurements indicate that sensor noise is dominated by field-dependent $1/f$ noise caused by magnetization fluctuations. Finally, a noise level as low as $1 \text{ nT/Hz}^{1/2}$ has been obtained. © 2002 American Institute of Physics. [DOI: 10.1063/1.1507818]

I. INTRODUCTION

Magnetoresistive devices are seeing increased use in a wide range of applications, i.e., as field sensors, position and rotation detectors, and as velocity sensors. Presently, most commercial magnetic sensors are based on the Hall effect, anisotropic magnetoresistance (AMR) effect,¹ or giant magnetoresistance (GMR) effect.² The more sensitive AMR and GMR sensors have magnetoresistance (MR) ratios less than 15% in such applications. In addition, all these sensors offer limited flexibility in electrical design. For example, the AMR and GMR devices tend to have resistance R values limited to a relatively narrow range. Since the discovery of large MR at room temperature,^{3,4} magnetic tunnel junctions (MTJs) have been extensively studied in past years. MTJs typically consist of two ferromagnetic (FM) layers separated by an insulating barrier. The value of resistance R depends on barrier thickness ($t \sim 0.5\text{--}2$ nm) exponentially and on junction area A inversely. Therefore, the junction resistance R can be varied easily over a wide range ($10^{-2}\text{--}10^8 \Omega$), while preserving the large MR ratio. The ability to tailor R in MTJs to suit the application therefore surpasses that in GMR devices. In addition, by choosing FM layers with large spin polarizations and optimizing growth conditions, MR ratios as high as 40%–50% are achievable at small fields.^{5,6} These properties have made MTJs promising candidates for use as ultrasensitive magnetic field sensors, and there has been some progress on developing a type of sensor based on MTJs.⁷

An ideal magnetic sensor should have linear field response and be free of hysteresis, which requires coherent rotation of magnetization under an external magnetic field. This can be done by utilizing the shape anisotropy of the free sensing electrode,⁸ or by introducing a transverse bias field, internally or externally,⁹ to achieve a single-domain state in the free electrode. Another issue in field sensing is that the intrinsic magnetic and electric noise of sensors be as low as possible. The field-sensing ability of MTJs is complicated by many noise sources; these include Johnson-Nyquist noise

(limited by resistance and temperature), shot noise, Barkhausen noise (due to domain-wall movement), and $1/f$ noise, which is dominant at low frequencies. For sensing applications, it is paramount that one characterizes the magnetic and electric noise in MTJ sensors. In this work, we present a study on the magnetic sensing response of MTJs under the influence of a variable hard-axis bias field. The MTJ sensors have a MR ratio of 35% and sensitivity of 3.5%/Oe at an optimal bias field. We have also characterized the noise spectra and explored the magnetic origin of the $1/f$ noise in our sensors. A noise level of $1 \text{ nT/Hz}^{1/2}$ has been obtained.

II. EXPERIMENTAL DETAILS

The layer structure of our MTJs consists of a buffer layer (300 Å Pt), a seed layer (30 Å Py), a pinning antiferromagnetic layer (130 Å FeMn), a bottom pinned electrode (60 Å Py), an insulator layer (Al_2O_3), a top free electrode (120 Å Py) and a capping layer (490 Å Al), in that order. Here Py stands for $\text{Ni}_{81}\text{Fe}_{19}$, a magnetostriction-free material. A schematic of the multilayer is shown in the inset of Fig. 1. All layers are deposited in a single process on SiO_2 -coated Si wafers via magnetron sputtering in a high vacuum chamber with a base vacuum of 2×10^{-8} Torr. A thin layer of Al with nominal thickness of 20 Å is deposited and subsequently plasma oxidized to form the Al_2O_3 tunnel barrier. An antiferromagnetic/FM pinning mechanism is used to provide exchange biasing¹⁰ for the bottom pinned electrode. To induce an easy direction in the free layer, a uniform magnetic field of 120 Oe is applied during sputtering. Optical lithography and Ar ion beam etching techniques are used for patterning junctions into rectangles with dimensions of $100 \times 150 \mu\text{m}^2$. Before measurement, samples are annealed at 170 °C for 3 min with a dc magnetic field (1.6 kG) parallel to the sample easy direction to improve exchange biasing and repair pinholes in the insulator.¹¹

III. RESULTS AND DISCUSSION

The magnetoresistance measurements were performed using a standard four-point dc measurement at room tem-

^{a)} Author to whom correspondence should be addressed; electronic mail: xiaoyong_liu@brown.edu

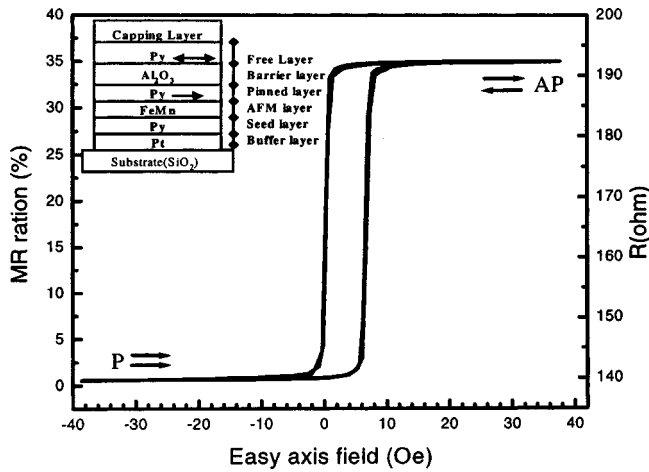


FIG. 1. Typical magnetoresistance of tunnel junctions as a function of easy-axis applied field. Coercivity of free layer is about 3 Oe. (Inset) Schematic view of our MTJ with bottom FM layer pinned via exchange bias. The arrows indicate the direction of applied field which biases the pinned layer and defines the easy axis of the free layer during deposition.

perature on a probe station equipped with two pairs of orthogonal electromagnets. This setup can provide field strengths of up to 200 Oe along the hard and easy axes. Because these fields are far smaller than the exchange bias field of our junctions, which is typically around 400 Oe,¹¹ only the magnetic response of the free layer need be considered. Figure 1 shows a typical MR curve with an external field applied along the easy axis of the sample. The two stable resistance states (140 Ω and 190 Ω respectively) correspond to antiparallel and parallel alignments of the magnetization in the free and pinned layers. MR ($\Delta R/R_p$, where R_p denotes the resistance in the parallel state) as high as 35% is obtained, implying a spin polarization of 0.38 for Py according to Julliere's two-current model.¹² This value is consistent with those reported in the literature.¹³ In spite of a few "Barkhausen" steps near the switching field, which are caused by the multidomain nature of the free layer, the magnetization reverses abruptly, indicating an irreversible process dominated by domain wall motion. The irreversibility of this transition suggests that it is inherently very noisy, a notion which is confirmed by low-frequency noise measurements.¹⁴

To obtain a favorable sensor response, it is necessary to create conditions in which the MTJ will switch its orientation via coherent rotation rather than by this highly hysteretic process. To this end, we have examined the easy-axis sensor response under the influence of a fixed external hard-axis (that is, perpendicular to the easy-axis) bias field. In the junctions we studied, the shape anisotropy and demagnetization field are negligible, due to relatively large junction sizes and small aspect ratios. The easy axis is therefore created by an anisotropy induced during deposition by the application of an external magnetic field, and it is also reinforced by following annealing process in the magnetic field applied along the easy axis. Figure 2 shows representative easy-axis response curves under different hard-axis bias fields. With the zero hard-axis field (Fig. 1), the MR curve is square with a coercivity of ~3 Oe, and the magnetic response is totally

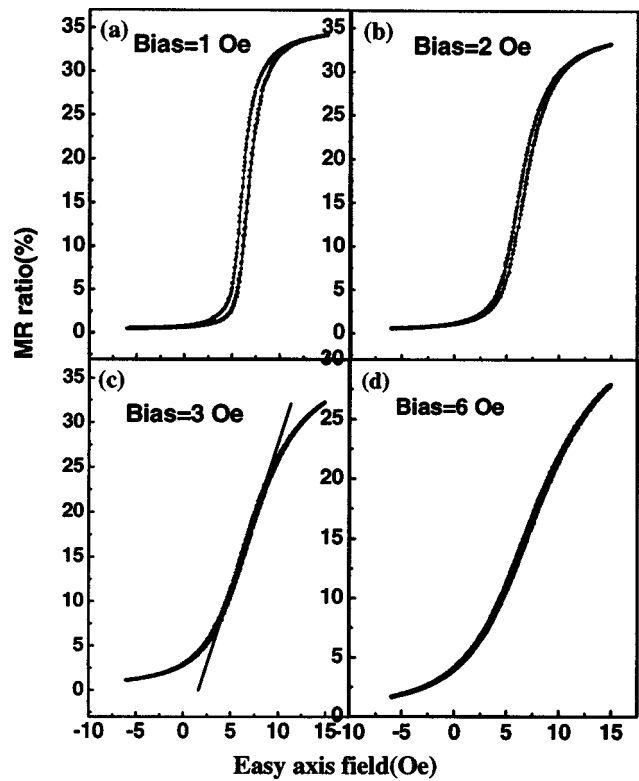


FIG. 2. MR loops of MTJs at different hard-axis bias fields.

governed by domain wall motion, which is irreversible and hence highly hysteretic. As a hard-axis field is introduced, the magnetoresistive response becomes more complicated, with the switching occurring through a combination of discontinuous jumps and coherent magnetization rotation, leading to decreased coercivity and a canting of the MR curve. As the bias field increases further, domain rotation becomes more and more significant and hysteresis decreases. For bias fields greater than 3 Oe, magnetization rotation dominates the behavior such that switching is coherent and reversible, with minimal hysteresis, and the MR is linear within a small field range. The slope, which determines the sensitivity of the sensor, is maximal at this critical point (~3.5%/Oe), and decreases slowly with increasing bias field.

In order to characterize the hysteresis of our samples, we have plotted the dependence of coercivity H_c on hard-axis bias field in Fig. 3. Here, H_c is defined as the half width of the hysteretic region of the MR curve. H_c is very sensitive to a small bias field. It drops abruptly from 3 Oe to less than 1 Oe upon the introduction of a bias field, and then decreases slowly as the bias field increases. It reaches a minimum of ~0.4 Oe when the bias field is 3 Oe, and maintains this value, with minor fluctuations (± 0.1 Oe), at higher bias fields. Our study shows that coercivity further decreases with decreasing easy-axis sweeping field range with no loss of sensitivity.

The above result can be interpreted by considering a uniformly magnetized free layer with uniaxial anisotropy $K \sin^2 \theta$ in a two-dimensional field. Here, K is the anisotropy constant and θ is the angle of magnetization with respect to the easy axis. Stoner and Wohlfarth (SW model)¹⁵ showed

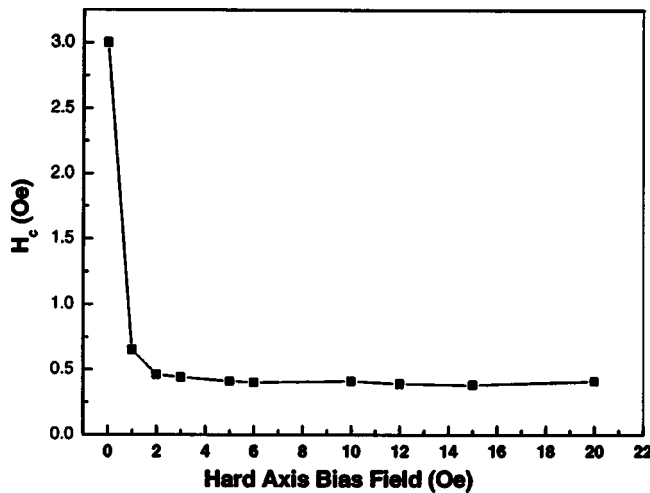


FIG. 3. Coercivity of MTJs as a function of hard-axis bias field with fixed easy field sweeping range ($-8 < H_x < 14$ Oe). Coercivity reaches a minimum value of 0.4 Oe in bias fields larger than 3 Oe.

that the theoretical shape of the critical, or "asteroid", curve for a single-domain particle is given by $H_x^{2/3} + H_y^{2/3} = (2 K/M)^{2/3}$, as shown in Fig. 4(a). H_x and H_y represent the easy- and hard-axis applied fields, respectively. As the hard-axis field increases, the magnetization rotates toward the hard axis. At the same time, the easy-axis switching field

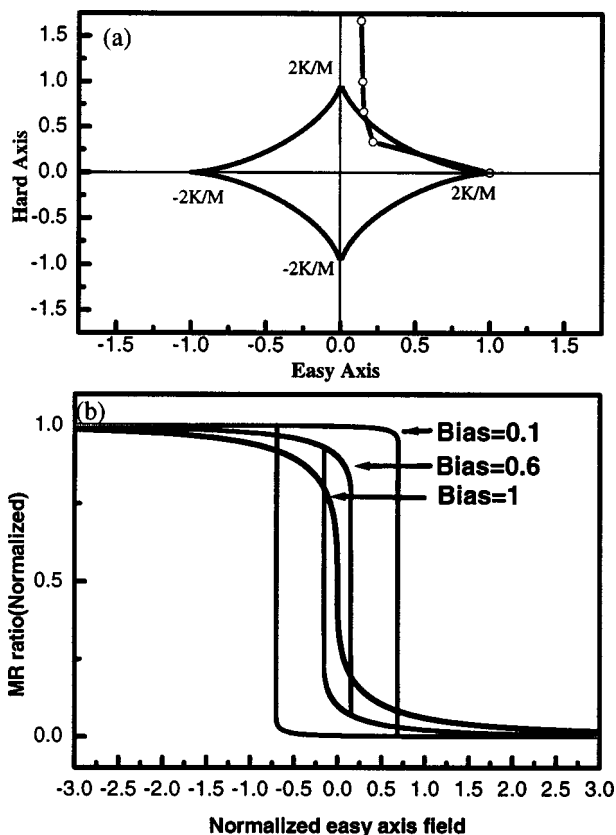


FIG. 4. (a) Stoner-Wohlfarth critical curve (asteroid) of a single domain particle with uniaxial anisotropy. For comparison, measured coercivity (normalized) is also shown (open circles). (b) Simulated MTJ response at different hard-axis bias fields. MR has been normalized with respect to MR ratio in the absence of bias.

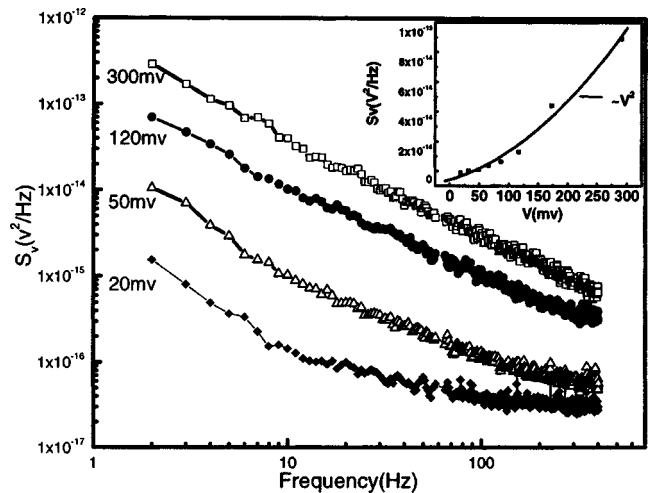


FIG. 5. Noise spectra of an MTJ sensor at different bias voltages in the absence of magnetic field. (Inset) Noise figure as a function of bias voltage. Noise increases as the square of the bias, as predicted by Hooge's law.

(H_c) begins to decrease from 2 K/M, which is the coercivity at zero bias field. It becomes zero when the hard-axis field is larger than 2 K/M, the effective uniaxial anisotropy field. The magnetoresistance of MTJs is related to the relative orientation of magnetization in the top and bottom FM layers, and is given by: $MR(\theta) = MR_0(1 - \cos \theta)/2$, where MR_0 is the magnetoresistance in the absence of a hard-axis bias. Utilizing these results, we have calculated normalized MR curves for various applied bias fields [Fig. 4(b)]. The calculations qualitatively agree with the experimental results, i.e., the magnetoresistance curve evolves from a square hysteresis loop at zero bias to an almost linear and nonhysteretic response when the bias field overcomes the sample anisotropy. According to the previous discussion, this critical field of 3 Oe corresponds to the effective easy-axis anisotropy field of the free layer, as is confirmed by the coercivity value obtained from Fig. 1. By assuming a magnetization of Py equal to that of the bulk material, we obtain a value of $K = 9 \times 10^3$ erg/cm³ for the anisotropy induced during deposition.

This SW model assumes a single-domain response. Our junctions have a multidomain structure in the free electrode and switching processes generally involve coherent rotation as well as domain wall motion, which might explain why H_c decreases much faster than expected from Fig. 4(a) with increasing hard-axis field. In addition, we neglected the interlayer coupling between electrodes, which would shift the MR curve along the easy axis. An interlayer coupling field of ~ 3.5 Oe is present in our junctions regardless of bias field. Sources of interlayer coupling in MTJ include orange-peel coupling¹⁶ and magnetostatic coupling. For our large junction sizes, the main mechanism is Néel coupling, which depends critically on barrier thickness and the roughness of the barrier interfaces.

To further explore the potential for sensor applications, we studied the low-frequency noise response of the MTJ sensors. We measured the noise power spectral density over the frequency range 1–400 Hz. A cross-correlation method was employed to extract the sensor noise from unwanted background and system noise. Figure 5 gives typical zero-

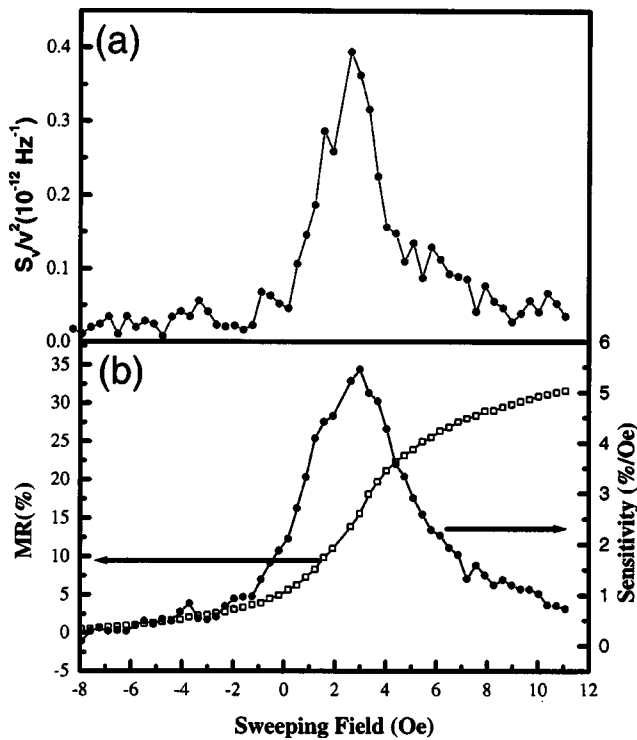


FIG. 6. (a) Noise figure at 1 Hz vs easy-axis field. (b) Corresponding MR curve and its derivative with respect to easy-axis field with a hard-axis bias of 5 Oe.

field noise spectra of junctions as the bias voltage applied across the MTJ device is varied. Within our measurement range, $1/f$ noise dominates the voltage noise S_v spectrum at frequencies below 100 Hz. The magnitude of $1/f$ noise increases as the square of bias voltage V in the range 10–300 mV as can be seen in the inset of Fig. 5, indicating that the noise is caused by resistance fluctuations in the junction and thus can be quantified by Hooge’s formula¹⁷ $S_v(f) = \alpha V^2/Nf^\gamma$, where α is a device-specific constant, N is the total number of fluctuators, and γ is in the range 0.6–1.4. Figure 6(a) shows the dependence of the normalized noise value S_v/V^2 at 1 Hz on easy-axis field for a typical sample, with a constant hard-axis bias of 5 Oe. For comparison, we also plotted the MR response and sensitivity of the sensor in Fig. 6(b). The noise increases substantially in the linear region, resulting a broad peak in the Néel field region. The roughly linear relationship observed between noise and sensitivity implies that this noise is dominated by thermally activated magnetization fluctuations in our sensors. This kind of magnetic noise has been previously observed in GMR¹⁸ and AMR¹⁹ sensors. The magnitude of magnetic field noise S_H is related to the voltage noise S_v by

$$S_H = \left(\frac{\partial H}{\partial V} \right)^2 S_v \approx \frac{1}{\left(\frac{1}{R} \frac{\partial R}{\partial H} \right)^2} \frac{S_v}{V^2}.$$

Using this definition, we estimate a magnetic noise level $S_H^{1/2}$ of about 1 nT/Hz^{1/2} with a sensitivity of 5%/Oe in a hard-axis bias field of 5 Oe.

IV. CONCLUSIONS

In summary, we have fabricated high quality Py/Al₂O₃/Py tunnel junction sensors with a magnetoresistance of 35%. Our study shows that the MR loop is very sensitive to an applied hard-axis field. Nonhysteretic sensor behavior can be obtained when the bias field exceeds the effective anisotropy induced during the deposition process, resulting in a linear response with a slope of 3.5%/Oe. Noise measurements have confirmed the magnetic origin of noise in our samples, and we have achieved a field noise level of 1 nT/Hz^{1/2}.

ACKNOWLEDGMENT

This work was supported the National Science Foundation Grant Nos. DMR- 0071770 and DMR-0074080.

- ¹T. R. McGuire and R. I. Potter, IEEE Trans. Magn. **MAG-11**, 1018 (1975).
- ²G. Binasch, P. Grunberg, F. Saurenbach, and W. Zinn, Phys. Rev. B **39**, 4828 (1989).
- ³J. S. Moodera, L. R. Kinder, T. M. Wong, and R. Meservy, Phys. Rev. Lett. **74**, 3273 (1995).
- ⁴N. Tezuka and T. Miyazaki, J. Magn. Magn. Mater. **139**, L231 (1995).
- ⁵S. S. P. Parkin, et al. J. Appl. Phys. **85**, 5828 (1999).
- ⁶X. F. Han, M. Oogane, H. Kubota, Y. Ando, and T. Miyazaki, Appl. Phys. Lett. **77**, 283 (2000).
- ⁷D. Lacour, H. Jaffrès, F. Nguyen Van Dau, F. Petroff, A. Vaurès, and J. Humbert, J. Appl. Phys. **91**, 4655 (2002).
- ⁸Y. Lu, R. A. Altman, S. A. Rishton, P. L. Trouillound, G. Xiao, W. J. Gallagher, and S. S. P. Parkin, Appl. Phys. Lett. **70**, 2610 (1997).
- ⁹M. Tondra, J. M. Daughton, D. Wang, R. S. Beech, A. Dink, and J. A. Taylor, J. Appl. Phys. **83**, 6688 (1998).
- ¹⁰J. Noguees and I. K. Schuller, J. Magn. Magn. Mater. **192**, 203 (1999).
- ¹¹X. Liu, C. Ren, L. Ritchie, B. D. Schrag, G. Xiao, and L. Li (unpublished).
- ¹²M. Jullière, Phys. Lett. **54A**, 225 (1975).
- ¹³R. Meservy and P. M. Tedrow, Phys. Rep. **238**, 174 (1994).
- ¹⁴S. Ingvarsson, G. Xiao, S. S. P. Parkin, W. J. Gallagher, G. Grinstein, and R. H. Koch, Phys. Rev. Lett. **85**, 3289 (2000).
- ¹⁵E. C. Stoner and E. J. Wohlfarth, Philos. Trans. R. Soc. London, Ser. A **240**, 599 (1948).
- ¹⁶L. Néel, C. R. Acad. Sci. III **255**, 1676 (1962).
- ¹⁷F. N. Hooge, Physica B **83**, 14 (1976).
- ¹⁸R. J. M. van de Veerdonk, P. J. L. Beliën, K. M. Schep, J. C. S. Kools, M. C. de Nooijer, M. A. M. Gijs, R. Coehoorn, and W. J. M de Jonge, J. Appl. Phys. **82**, 6152 (1997).
- ¹⁹H. T. Hardner, M. B. Weissman, M. B. Salamon, and S. S. P. Parkin, Phys. Rev. B **48**, 16156 (1993).